EUKARYOTIC CELL, Apr. 2008, p. 647–655 Vol. 7, No. 4
1535-9778/08/$08.00+0 doi:10.1128/EC.00411-07

Phenotype of a Mechanosensitive Channel Mutant, *mid-1*, in a Filamentous Fungus, *Neurospora crassa*▽

Roger R. Lew,[1]* Zohaib Abbas,[1] Marinela I. Anderca,[1] and Stephen J. Free[2]

Biology Department, York University, 4700 Keele Street, Toronto, Ontario M3J 1P3, Canada,[1] and Department of Biological Sciences, University of New York at Buffalo, Buffalo, New York 14260[2]

Received 8 November 2007/Accepted 12 February 2008

In the yeast *Saccharomyces cerevisiae*, the *MID1* (*m*ating-*i*nduced *d*eath) gene encodes a stretch-activated channel which is required for successful mating; the mutant phenotype is rescued by elevated extracellular calcium. Homologs of the *MID1* gene are found in fungi that are morphologically complex compared to yeast, both *Basidiomycetes* and *Ascomycetes*. We explored the phenotype of a *mid-1* knockout mutant in the filamentous ascomycete *Neurospora crassa*. The mutant exhibits lower growth vigor than the wild type (which is not rescued by replete calcium) and mates successfully. Thus, the role of the MID-1 protein differs from that of the homologous gene product in yeast. Hyphal cytology, growth on diverse carbon sources, turgor regulation, and circadian rhythms of the *mid-1* mutant are all similar to those of the wild type. However, basal turgor is lower than wild type, as is the activity of the plasma membrane H^+-ATPase (measured by cyanide [CN^-]-induced depolarization of the energy-dependent component of the membrane potential). In addition, the mutant is unable to grow at low extracellular Ca^{2+} levels or when cytoplasmic Ca^{2+} is elevated with the Ca^{2+} ionophore A23187. We conclude that the MID-1 protein plays a role in regulation of ion transport via Ca^{2+} homeostasis and signaling. In the absence of normal ion transport activity, the mutant exhibits poorer growth.

Stretch-activated (mechanosensitive) ion channels are known to play a role in the growth and development of hyphal organisms. In the urediniomycete *Uromyces appendiculatus* (37), the oomycete *Saprolegnia ferax* (7), the yeast *Candida albicans* (36), and the ascomycete *Neurospora crassa* (14), the presence of mechanosensitive ion channels has been demonstrated with the patch clamp technique. The roles of mechanosensitive channels in these hyphal organisms are different. In the rust fungus, *U. appendiculatus*, they function as a sensor of mechanical barriers during infection of the plant host (37); a similar thigmotropic response occurs in *C. albicans* (36). In *S. ferax*, stretch-activated channels function as sensors of cell expansion, mediating Ca^{2+} influx to maintain a tip-high Ca^{2+} gradient during hyphal extension (8). The latter role is also observed in tip-growing pollen tubes of higher plants (5), but cannot be considered universal, since the filamentous fungus *N. crassa* relies upon an endomembrane IP_3-activated Ca^{2+} channel to maintain a tip-high Ca^{2+} gradient during hyphal extension (33) rather than stretch-activated channels (14).

The *MID1* gene of the yeast *Saccharomycese cerevisae* encodes a stretch-activated nonselective cation channel, based on patch clamping after heterologous expression in mammalian CHO cells (11). Mid1p is required for Ca^{2+} influx and projection (shmoo) formation during mating in yeast (10). The gene is ubiquitous among fungal organisms. A BLAST search revealed homologous sequences in other yeasts, as well as both ascomycete and basidiomycete filamentous fungi (unpublished observation). Notably, there is a cysteine-rich region which is highly conserved and is required for function (24). A MID1 homolog from the higher plant *Arabidopsis thaliana* (Mca1) was cloned on the basis of functional complementation of the yeast mid1 mutant, and appears to function in Ca^{2+} influx and thigmotropism in plants (26). In yeast, both MID1 and a homolog of a voltage-dependent Ca^{2+} channel in higher eukaryotes (CCH1) appear to function together in Ca^{2+} uptake (29). Brand et al. (3) found that both CCH1 and MID1 contribute to Ca^{2+} influx and thigmotropic responses in *C. albicans*.

Our objective was to explore the role of MID1 in a filamentous fungi, *Neurospora crassa*. A *mid-1* knockout was obtained from the *Neurospora* Genome Project (4). The *mid-1* gene (NCU06703.3) in *N. crassa* is 24% identical and 40% similar to the *S. cerevisiae MID1* gene. Homology is strongest in a region of nine conserved cysteines which has been identified as required for function in *S. cerevisae* (24), a region which is highly conserved in alignments of homologous sequences from other fungi (unpublished observation). Lower homology is observed in the N-terminus region encoding four hydrophobic segments (H1 to H4) required for localization of the *S. cerevisiae* Mid1p to the endoplasmic reticulum and plasma membrane (28).

There are two stretch-activated Ca^{2+}-permeable channels in the *N. crassa* plasma membrane (14). The channels do not function in tip growth, since inhibition of the channels with gadolinium induced only transient arrest of hyphal extension. To determine what role a stretch-activated channel could have in *N. crassa*, we explored the phenotype of the *mid-1* mutant under a range of physiological conditions: carbon requirements, mating and developmental pathways, barrier responses, electrical properties, Ca^{2+} homeostasis, and turgor regulation. The *mid-1* mutant exhibits low growth vigor compared to the wild type under all conditions tested, pointing to a pleiotropic effect on growth of the filamentous fungi. The mutant is hypersensitive to low extracellular [Ca^{2+}] and high intracellular

* Corresponding author. Mailing address: Department of Biology, York University, 4700 Keele Street, Toronto, Ontario M3J 1P3, Canada. Phone: (416) 736-5243. Fax: (416) 736-5698. E-mail: planters@yorku.ca.

▽ Published ahead of print on 22 February 2008.

[Ca^{2+}] and exhibits low turgor and a depolarized electrical potential (attributable to low H^+-ATPase activity) compared to the wild type. Thus, the poor growth vigor of the mutant appears to have its foundation in Ca^{2+} regulation of ion transport.

MATERIALS AND METHODS

Strains. Stock cultures of wild type (strain 74-OR23-1A, FGSC no. 987; strain 74-OR23-1VA, FGSC no. 2489; and strain 74-ORS-6a, FGSC no. 4200), and the *mid-1* mutant (NCU06703.2, mating type *A*, FGSC no. 11708; and mating type *a*, FGSC no. 11707) were obtained from the Fungal Genetics Stock Center (School of Biological Sciences, University of Missouri, Kansas City) (25). Using PCR amplification of the genomic DNA, we verified the insertion of the hygromycin resistance gene into the *mid-1* gene at the site predicted from the primer sequences published by the *Neurospora* Genome Project (www.dartmouth.edu/~neurosporagenome/) to create the knockout *mid-1* mutant (4). Cultures were maintained on Vogel's minimal medium (35) plus 1.5% (wt/vol) sucrose and 2.0% (wt/vol) agar (VM).

Growth measurements. For various media and conditions described in the Results section, growth was normally measured by placing either conidia or a plug of agar containing mycelium in the center of a petri dish and colony diameter was measured every 2 to 3 h to obtain linear rates of diameter increase over a period of 20 to 24 h. Some experimental replicates used race tubes to extend the period of growth to 96 h. In both cases, growth rates were calculated as cm h^{-1}. Fresh-weight comparisons were performed by growing colonies on cellophane in larger (15 by 150 mm) petri dishes, measuring colony diameter, and harvesting the mycelium for fresh-weight measurements after 16, 23, and 36 h of incubation. For growth in agar of various hardnesses, conidia were placed in the center of the petri dish and covered with dialysis tubing. Colony growth measurements were performed at 28°C unless stated otherwise. The extension rates of hyphal tips, either on the surface or embedded in the agar, were measured using 2-min time-lapse microphotography for 18 min at room temperature (22 to 24°C). Measurements were performed at the four compass points of the colony.

Culture preparation for electrical and turgor experiments. Conidia were transferred onto strips (2.5 by 6 cm) of cellophane dialysis tubing that overlay the VM in petri dishes and incubated overnight at 28°C (or room temperature, 21 to 24°C). Prior to the experiment, the cellophane was cut with a razor blade to a size of about 1 by 3 cm, which included the growing edge of the colony. The cellophane strip was placed inside the cover of a 30-mm petri dish and immobilized on the bottom with masking tape. The culture was flooded with 3 ml of buffer solution (BS): 10 mM KCl, 1 mM $CaCl_2$, 1 mM $MgCl_2$, 133 mM sucrose, and 10 mM MES (morpholineethanesulfonic acid), pH adjusted to 5.8 with KOH. Growth of hyphae at the colony edge normally resumed within 15 min. We usually interspersed measurements of the mutant (FGSC 11708) and wild-type (FGSC 2489 or 987) strains.

Electrical measurements. Large trunk hyphae (10 to 20 μm diameter) about 0.5 cm behind the colony edge were selected for electrophysiology measurements. Double-barrel micropipettes were prepared as described by Lew (18). After impalement, the membrane potential usually stabilized within 2 to 3 min, and then the voltage clamp was performed (17). Briefly, current injection and voltage monitoring through the two barrels of the micropipette were used to voltage clamp the hyphae using a bipolar staircase of resting potential and alternating positive and negative voltage clamps with a duration of 50 ms. Measurements of current density in the hyphae are complicated by the cable properties of the hypha. Voltage is attenuated about 67% at a distance of about 400 μm from the site of micropipette impalement (19). Correction for current spread along the hypha requires multiple impalements, technically challenging because vibration during treatments may dislodge the micropipettes. Thus, input currents are shown.

Turgor measurements. Similarly to electrophysiological measurements, large trunk hyphae were selected about 0.5 cm behind the growing edge of the colony for turgor measurements (20, 21). Large-aperture micropipettes were fabricated using a double-pull technique and filled with low-viscosity silicon oil (polydimethylsiloxane, 1.5 centistokes; Dow Corning, Midland, WI). The micropipette was mounted in a holder attached to a micrometer-driven piston by thick-wall Teflon tubing. The internal hydrostatic pressure of the hypha causes the silicon oil/cell sap meniscus to move into the micropipette after impalement; the pressure required to bring the meniscus back to the tip is a measure of the turgor. Pressure was measured with a transducer (XT-190-300G; Kulite Semiconductor, Leonia, NJ) mounted on the holder. To assure that the probe tip had not become plugged, the meniscus was periodically drawn back from the tip and then returned to the tip. Turgor was measured for about 6 min (a total of six or seven measurements). For turgor recovery measurements, after turgor measurements for about 6 min, 0.5 ml of BS plus 1,000 mM sucrose was added to the dish containing 3 ml of BS for a hyperosmotic increase of about 155 mosmol kg^{-1}. If the micropipette tip became plugged during the turgor measurements or the hypha became damaged, other hyphae nearby were impaled with a fresh micropipette.

Microscopy. For electrical, turgor, and hyphal tip growth measurements, a Zeiss Axioskop 2 microscope (Carl Zeiss Canada, Don Mills, Ontario, Canada) was used with a ×40 objective (water immersion, numerical aperture 0.8) or a ×10 objective. Hyphal tip morphology was imaged using bright-field, differential interference contrast (DIC) or epifluorescence (Mito Fluo Red and FM4-64; Molecular Probes) with a ×100 objective (EC Plan Neofluar oil immersion, numerical aperture 1.3). Digital images were captured with an Orca C-4742-95 camera (Hammamatsu Photonics KK, Japan) using OpenLab 3.1.7 software (Improvision, Coventry, United Kingdom). Chlortetracycline fluorescence was imaged on an Olympus confocal microscope (×60 oil immersion objective) using Fluoview software as previously described (15).

Circadian rhythm measurements. A *csp-1*; *bd*; *mid-1* mutant was constructed for determination of the circadian conidiation rhythm by crossing the *mid-1* knockout mutant to *csp-1*; *bd* using standard crossing techniques. The mutant was grown in race tubes on VM with 0.5% (wt/vol) maltose, 0.01% (wt/vol) arginine, and 2% (wt/vol) agar (12) at 22°C. Initially, it was grown under constant light for 24 h and then transferred to continuous darkness. The growth front was measured every 24 h under a red safelight. After 1 to 2 weeks, the conidial banding patterns were determined and periodicity was quantified by reference to growth rate (13).

Gene expression. Reverse transcription-PCR (RT-PCR) was used to confirm that the wild-type *mid-1* gene is expressed in *N. crassa*. RNA was isolated from liquid nitrogen-ground mycelia using the TRIzol reagent (Invitrogen, Carlsbad, CA), and mRNA was enriched with the PolyATract mRNA isolation system IV (Promega, Madison, WI). The poly(A)$^+$-enriched RNA was transcribed with Moloney murine leukemia virus reverse transcriptase (New England Biolabs Ltd., Ontario, Canada) for 90 min at 37°C and then subjected to PCR cycling with *N. crassa* gene-specific primers. The primers NcMid-RT1f (TAAGCAGC AGTTCTTCTTCAGCG) and NcMidm-RT2r (AATTGAACCCCTTCTGGCC AGGC) were designed to cover a fragment of 782 bp from the *mid-1* cDNA, while the positive control was provided by a β-tubulin 651-bp fragment obtained with primers NcTUB1f (AACTTACAAGATGGCAGAGC) and NcTUB2r (A AGGGGTCACTACACTGAGGG). For RT-PCR, the Qiagen OneStep RT-PCR kit (Hilden, Germany) was used with either 66 or 6.6 ng of mRNA. Additional controls without mRNA or mRNA added after the transcription step established the absence of contamination (not shown). Band intensities were quantified using integrated density measurement in ImageJ (developed at the National Institutes of Health and available at http://rsb.info.nih.gov/ij.).

Statistical analysis. Data are shown as means ± standard deviation (sample size), unless stated otherwise. Statistical significance was usually determined using two-tailed *t* tests (Microsoft Excel) or, as noted, nonparametric tests (SYSTAT, Inc., Evanston, IL).

RESULTS

The *mid-1* gene is expressed in the wild type. RT-PCR of isolated mRNA showed that the *mid-1* gene product is expressed in the wild type. The level of expression was about 0.44-fold less than that of a β-tubulin mRNA (assuming that the PCR amplification efficiencies of *mid-1* and β-tubulin mRNAs are equivalent) (data not shown). Thus, the gene is expressed in growing mycelia of the wild type.

General growth characteristics. The *mid-1* mutant exhibited consistently lower growth rates than the wild type. When grown as colonies overlying cellophane in petri dishes for 36 h, the colony diameter increased 0.295 ± 0.009 cm h^{-1} and 0.453 ± 0.018 cm h^{-1}, while the fresh-weight increases were 21 and 45 mg h^{-1}, respectively ($n = 3$). The smaller colony size of *mid-1* was partially offset by a higher colony density (1.16 ± 0.22 mg cm^{-2}) than that of the wild type (1.04 ± 0.22 mg cm^{-2}) ($n = 3$). The *mid-1* mutant had a higher branching density based on

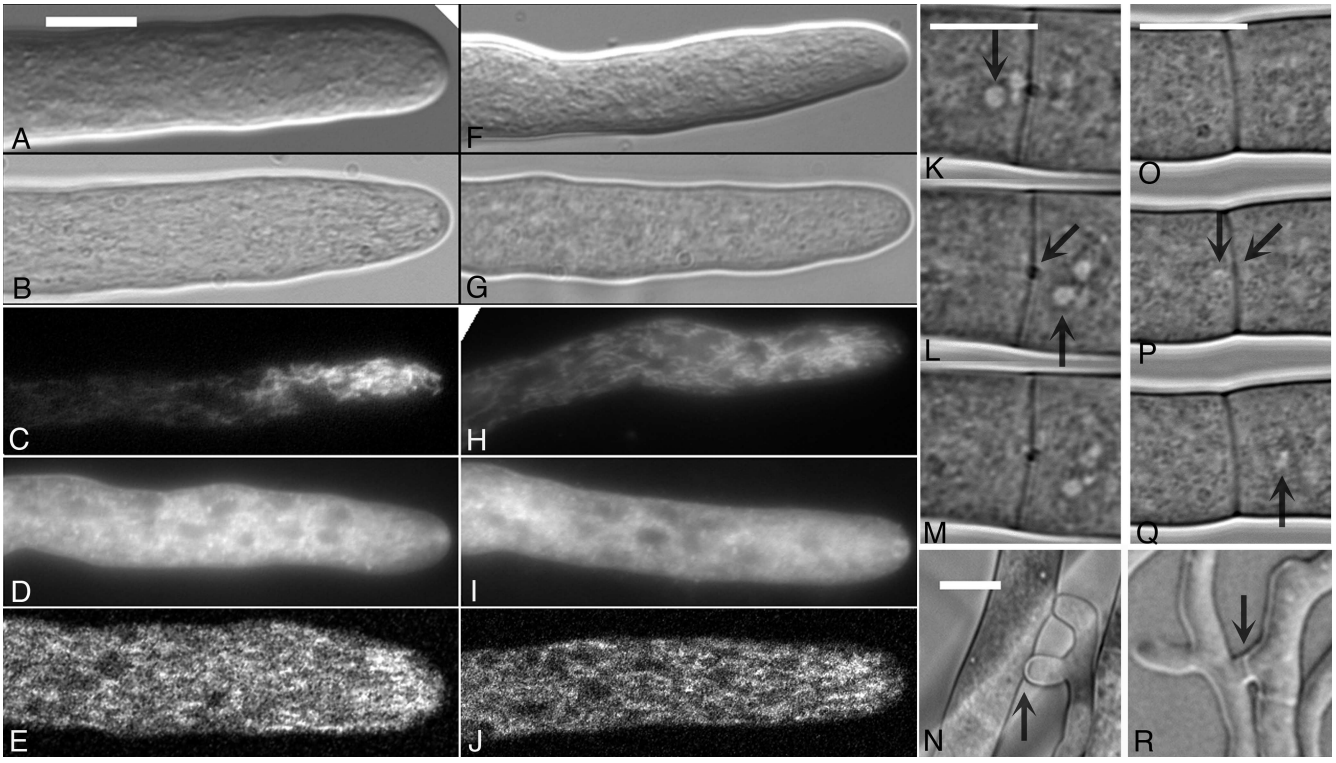

FIG. 1. Hyphal morphology and cytology of the wild type and the *mid-1* mutant. Wild-type images are shown in the left panels (A to E and K to N); *mid-1* mutant images are shown in the right panels (F to J and O to R). Images of growing hyphal tips were taken with a ×100 objective (oil immersion), either on a microscope slide (DIC imaging) (A and F) or on agar, covered with a coverslip (bright-field imaging) (B and G) or after incubation with the mitochondrion-specific fluorescent dye Mito Fluo Red (C and H), the membrane-specific fluorescence dye FM4-64 (D and I), or the Ca^{2+}-sensitive dye chlortetracycline (E and J). Mitochondria exhibit a tip-high distribution, as reported previously (15). Compared to Mito Fluo Red-fluorescing mitochondria, the membrane-specific FM4-64 fluorescence is distributed further behind the tip and at the tip, in the Spitzenkorper. Chlortetracycline exhibits a tip-high distribution, consistent with a previous report that it is mostly colocalized with mitochondria (15). Oblate to spherical zones of fluorescence exclusion behind the tip are assumed to be caused by nuclei. Hyphal flow of the wild type (K to M) and the *mid-1* mutant (O to Q) was imaged with a ×100 objective (oil immersion) by placing a coverslip on the growing edge of a colony growing on agar. The trunk hyphae were within 500 μm of the growing colony edge. The images were taken every 1 s. Vertical arrows point to organelles moving toward the colony edge which have passed through the septal pore in the center of the septa (diagonal arrows) during the 3-s duration shown. Images of anastomoses (hyphal fusions) were taken with a ×40 objective (water immersion) of mycelium sandwiched between two layers of cellophane overlying agar. Vertical arrows point to the fusion points through which hyphal flow was observed in both the wild type (N) and the *mid-1* mutant (R). Bars, 10 μm.

measurements of the hyphal growth unit (hyphal length/number of branches) (34). The *mid-1* mutant had a hyphal growth unit of 56 ± 17 μm ($n = 25$), considerably lower than that of the wild type (116 ± 24 μm; $n = 14$). When measured as linear extension in race tubes for 96 h, growth rates of the *mid-1* mutant and wild type were 0.11 cm h^{-1} and 0.35 cm h^{-1}, respectively. In liquid cultures inoculated with 0.31×10^6 conidia, the *mid-1* mutant growth was similar to that of the wild type after 44 h of incubation (8.2 ± 0.4 mg h^{-1} and 7.9 ± 1.3 mg h^{-1}, respectively; $n = 3$). In addition to the slower colony growth on agar, the *mid-1* mutant produced fewer conidia when grown in slants. The mycelial architecture behind the growing colony edge was denser and less organized than that of the wild type, with poorly defined main trunk hyphae and interconnecting fusion hyphae (1). To assess whether poor growth was caused by disarranged cytological architecture, we examined hyphal cytology in detail.

Tip cytologies are similar in the wild type and the *mid-1* mutant. Hyphal tip morphologies are similar when imaged with DIC or bright-field imaging of growing hyphae (Fig. 1). The fluorescent dyes Mito Fluo Red and FM4-64 were used to image mitochondria (15) and endomembranes (6), respectively. Both dyes exhibited similar distributions in the wild type and the mutant (Fig. 1). Mitochondrial distribution can be considered an indirect measure of cytoskeletal structure, since disruption of microtubules with nocadazole modifies mitochondrial distributions (15); thus, microtubular architecture appears to be unaffected in the *mid-1* mutant. The distribution of nuclei, observed as spherical or oblate regions of fluorescence exclusion in hyphae stained with Mito Fluo Red and FM4-64, were similar as well, also consistent with a fully functional cytoskeleton (31). In the expectation that Ca^{2+} homeostasis may be disrupted in the *mid-1* mutant, we examined Ca^{2+} sequestration in mitochondria with chlortetracycline (15), which exhibited similar tip-high distributions in both the wild type and the *mid-1* mutant (Fig. 1).

Hyphal flow was observed in both the wild type and the *mid-1* mutant, and the rates were qualitatively similar (Fig. 1). Anastomoses (hyphal fusions) (9) formed in both strains as well (Fig. 1). Because of the high mycelial density of the *mid-1*

mutant compared to the wild type, no quantitative comparisons were attempted. There was no qualitative difference in the formation of anastomoses and hyphal flow through them.

Carbon source does not affect *mid-1* growth. Another general cause of poor growth could be nutrient utilization. The following carbon sources were tested in preliminary experiments (in VM plus 2% agar): 0.75% (wt/vol) glucose, 1.5% (wt/vol) sucrose, 1.5% (wt/vol) maltose, 2.38% (wt/vol) raffinose, 0.75% (wt/vol) dextrin, 1.5% (wt/vol) starch, 1.5% (wt/vol) glycogen, 0.37% (wt/vol) glycerol, and 1.13% (wt/vol) oleic acid. Growth rates of the wild type varied from 0.15 cm h^{-1} on glycogen to 0.24 cm h^{-1} on glucose. The *mid-1* mutant's growth rate ranged from 0.08 cm h^{-1} on glycerol to 0.12 cm h^{-1} on starch. The mutant growth rate was consistently lower than the wild-type growth rate on the same media, ranging from 44% on oleic acid and glycerol to 71% on glycogen. The lower growth rate of the *mid-1* mutant was independent of the carbon source. To test for a micronutrient requirement, VM was supplemented with 1% yeast extract (Difco). Growth rates of the wild type were 0.26 (25°C) and 0.37 (37°C) cm h^{-1} in VM and 0.25 (25°C) and 0.34 (37°C) cm h^{-1} in VM supplemented with 1% (wt/vol) yeast extract. The *mid-1* mutant growth rates were 0.13 (25°C) and 0.22 (37°C) cm h^{-1} in VM and 0.07 (25°C) and 0.21 (37°C) cm h^{-1} in VM plus yeast extract. Thus, the lower growth rates of the *mid-1* mutant are not due to a requirement for a micronutrient or metabolite supplied in yeast extract.

Circadian rhythms are unaffected in the *mid-1* mutant. Given the general phenotype of low vigor in the *mid-1* mutant—low growth rates and poor production of conidia compared to the wild type—we tested the genetic control of developmental pathways by comparing the circadian rhythms of the mutant and wild type. (Experiments were performed at 22°C.) The *mid-1* mutant (*csp-1*$^+$; *bd*$^+$; *mid-1*$^-$) was crossed with the *csp-1 bd* mutant (*csp-1*$^-$; *bd*$^-$; *mid-1*$^+$). Selection for *csp-1*$^-$ was performed using the tap test to demonstrate the absence of conidial spore release. Selection for *csp-1*$^-$; *bd*$^-$; *mid-1*$^-$ was based on the mutant's lower growth rate. The *csp-1*$^-$; *bd*$^+$; *mid-1*$^+$ mutant's growth rate was 0.29 ± 0.03 cm h^{-1} ($n = 5$). The *csp-1*$^-$; *bd*$^-$; *mid-1*$^+$ mutant's growth rate was 0.15 ± 0.02 cm h^{-1}, and the circadian period was 20.1 ± 0.6 h ($n = 3$). The *csp-1*$^-$; *bd*$^+$; *mid-1*$^-$ mutant's growth rate was 0.12 ± 0.02 cm h^{-1} ($n = 5$). (The circadian period could not be determined in the *bd*$^+$ genotype.) The *csp-1*$^-$; *bd*$^-$; *mid*-1$^-$ mutant's growth rate was 0.11 ± 0.01 cm h^{-1}, and the circadian period was 21.7 ± 0.5 h ($n = 6$). Thus, in spite of the lower growth rate of the *mid-1* mutant, circadian rhythms and the timing of the conidiation developmental pathway are unaffected.

The *mid-1* mutant is viable after mating. In *S. cerevisiae*, the *mid1* mutant is unable to mate. In *N. crassa*, viability of ascospores was assessed with the following permutations of crosses (male on the left): *mid-1 A* (FGSC 11708) × *mid-1 a* (FGSC 11707); *mid-1 a* (FGSC 11707) × *mid-1 A* (FGSC 11708); and control matings of the *A* and *a* wild types (FGSC 2489 and 4200, respectively). In all instances, ascospore viability was about 100%. Therefore, unlike the *S. cerevisiae mid1* mutant, mating is unaffected in *N. crassa*.

Low extracellular calcium inhibits *mid-1* growth. In yeast, the mating-induced death phenotype is rescued by elevated Ca^{2+}. To test for calcium rescue of the low growth rate of the *N. crassa mid-1* mutant, yeast extract-peptone-dextrose medium (YEPD) was used, with or without 25 mM $CaCl_2$ supplement in extended measurements (90 h) using race tubes. The *mid-1* mutant grew more slowly than the wild type without the Ca^{2+} supplement (0.16 compared to 0.37 cm h^{-1}) and was unaffected by Ca^{2+} addition (0.16 compared to wild-type growth of 0.31 cm h^{-1}) ($n = 2$ or 3). To test for a calcium requirement for growth, the two strains were grown on YEPD containing the Ca^{2+} chelator BAPTA at 0.2 to 1.0 mM. At 1.0 mM BAPTA, free [Ca^{2+}] in YEPD is depleted to 100 nM compared to its normal concentration of 0.14 mM in the absence of BAPTA (23). Wild-type growth was affected only slightly when free Ca^{2+} was decreased with 1.0 mM BAPTA. In contrast, the *mid-1* mutant was unable to grow at 1.0 mM BAPTA (Table 1). Growth rates were near normal when the 1.0 mM BAPTA medium was supplemented with 1.1 mM Ca^{2+}, indicating that the BAPTA effect was due to Ca^{2+} chelation.

TABLE 1. Ca^{2+} dependence of growth

BAPTA concn (mM)	Growth rate (cm h^{-1})[a]	
	Wild type	*mid-1* mutant
0	0.523 ± 0.006	0.219 ± 0.003
0.2	0.493 ± 0.012	0.211 ± 0.011
0.6	0.494 ± 0.015	0.174 ± 0.006*
1.0	0.415 ± 0.025*	0.008 ± 0.006*
1.0 + 1.1 mM $CaCl_2$	0.505 ± 0.028	0.214 ± 0.010

[a] Data are shown as means ± standard deviations for three independent replicates. Two-tailed *t* tests were performed relative to the control growth rate with 0 mM BAPTA. *, significantly different from the control growth rate ($P < 0.02$).

Elevation of intracellular calcium inhibits *mid-1* growth. To test the effect of intracellular Ca^{2+} on the mutant, we first attempted direct injection using ionophoresis. The large trunk hyphae were impaled with a double-barrel micropipette and a single-barrel micropipette containing either 25 mM Ca^{2+} or BAPTA for ion injection located further behind the colony edge, so that mass flow would move the Ca^{2+} or BAPTA toward the double-barrel micropipette. For either Ca^{2+} or BAPTA injections (1 to 5 nA), the potential depolarized slightly (data not shown). Due to the large volume of the hyphae and the complication of hyphal flow dispersing the injected Ca^{2+} or BAPTA, the extent to which cytoplasmic Ca^{2+} was affected is uncertain. So an alternative method for elevating intracellular Ca^{2+} was used: the calcium ionophore A23187, which is known to increase intracellular Ca^{2+} based on increased aequorin fluorescence in *Aspergillus awamori* (27). The ionophore (10 μl from a 9.5 mM stock in ethanol) was spotted onto the YEPD agar plate (Fig. 2). The wild type grew through the circular zone containing the A23187 ionophore, exhibiting hyperbranching from the hyphal tips, a phenomenon previously reported by Reissig and Kinney (30), and along hyphal trunks within the ionophore zone. Conidiation was absent after 1 to 2 days, in a sector extending back to the inoculum, but was observed elsewhere on the plate, including the control zone in which 10 μl of ethanol had been applied (Fig. 2A). The mutant *mid-1* did not grow in the ionophore zone at all (Fig. 2B and F). Thus, calcium homeostasis is

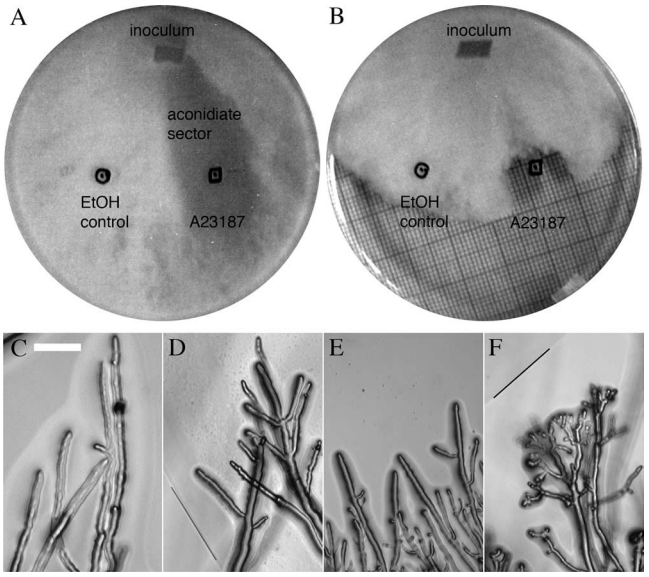

FIG. 2. Ca^{2+} ionophore effects on growth of the wild type and the *mid-1* mutant. The strains were inoculated by transferring an agar block (inoculum) onto petri dishes (YEPD plus 2% agar) on which either the Ca^{2+} ionophore (10 μl of 9.5 mM A23187 in ethanol [in boxes]) or ethanol (10 μl [in circles]) had been spotted. The petri dishes were photographed bottom side up (on top of graph paper) after 38 h of growth. Note that the wild-type strain grew through A23187 but did not conidiate in a sector extending back to the inoculum (A). The *mid-1* mutant did not grow into the A23187 zone (B). The responses of individual hyphae are shown in panels C through F. The wild type was unaffected by the ethanol control (C); upon entering the A23187 zone, it hyperbranched (D [the border of the A23187 zone is marked by a line]). The *mid-1* mutant was also unaffected by ethanol (E) but hyperbranched and stopped growth prior to entry into the A23187 zone (F [the border of the zone is marked by a line]). The petri dish diameters are 90 mm, and the microphotograph scale bar is 100 μm.

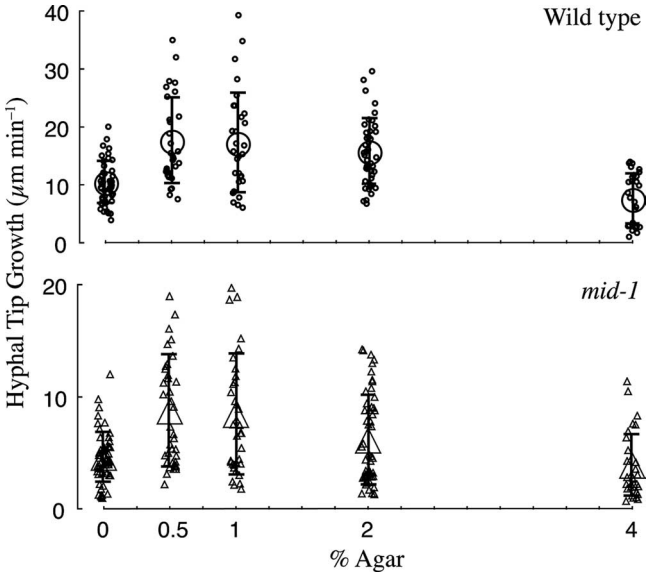

FIG. 3. Hyphal penetration through agar. Mycelial colonies were grown in substrates of various hardnesses (0.5 to 4.0% [wt/vol] agar) or submersed (0% agar). In all cases, the growth medium was VM supplemented with 1.5% (wt/vol) sucrose. Growth of hyphal tips at the four compass points of the colony edge was measured for 18 min, and average growth rates were calculated. For 0% agar, colonies growing on 2% agar were flooded with VM and then hyphae growing above the agar surface (but submersed in VM) were measured. Data are jittered on the *x* axis for clarity. Both the wild type (upper panel) and the *mid-1* mutant (lower panel) exhibited a similar response to increasing substrate hardness. In all cases, *mid-1* growth was lower than wild-type growth.

affected in the *mid-1* mutant. Compared to the wild type, the mutant is more sensitive to lower extracellular Ca^{2+} and elevated cytoplasmic Ca^{2+}. As a Ca^{2+}-permeant mechanosensitive channel, the MID-1 protein may function in signaling required by the growing hyphae to respond to mechanical impediments.

Mechanical impedance has similar effects on *mid-1* mutant and wild-type growth. Hyphal growth through media of various hardnesses was examined by measuring the growth rate of hyphae embedded in 0 to 4% agar (Fig. 3). Although we did not measure agar "hardness" directly, viscosity increases from 0.8×10^6 to 52×10^6 cP as the agar concentration is increased from 1 to 4% (wt/vol) at 46°C (32). (Water viscosity is 1 cP.) Thus the increase in "hardness" as agar concentration is increased from 0.5 to 4% (wt/vol) should be dramatic. Both strains exhibit similar responses to agar "hardness": embedded hyphal growth rates were highest at 0.5 to 1.0% (wt/vol) agar, declining about 45% in 4% (wt/vol) agar. The growth of the *mid-1* mutant was consistently lower, ranging from 38% to 51% of the wild-type growth rate.

To examine the response of hyphae to mechanical barriers (thigmotropism), in initial experiments, colonies were grown on VM sandwiched between layers of scratched dialysis tubing and time-lapse imaging was used to screen for instances of hyphal growth into an obstruction at the growing colony edge. This technique mimics a more sophisticated approach to characterize thigmotropism in the yeast *Candida albicans*. Brand et al. (3) adhered *C. albicans* yeast cells to polylysine-coated quartz slides with specially produced 0.79-μm ridges, immersed the slides in serum to induce pseudohyphal growth, and quantified hyphae reorienting upon contact with a ridge. In *N. crassa*, apical branching responses were observed in both the wild type and the *mid-1* mutant upon contact with the obstructions created by scratching the dialysis tubing (data not shown). For quantitative measurements, a micropipette tip was appressed onto the hyphal tip. Multiple examples of apical branching were observed for both the wild type (16/21 experiments) and the *mid-1* mutant (17/19 experiments) (examples shown in Fig. 4). Thus, responses to mechanical impediments were the same in the wild type and the *mid-1* mutant.

***mid-1* turgor is lower than wild type.** Besides responses to mechanical impediments, stretch-activated channels may function in osmotic responses (since changes in extracellular osmolarity will cause either swelling or shrinking of the hyphae), so turgor relationships were examined.

In interspersed measurements of the *mid-1* mutant and wild type, turgor of the mutant was 400 ± 97 kPa ($n = 17$) while that of the wild type was 530 ± 67 kPa ($n = 15$) (Fig. 5); the difference was statistically significant (two-tailed t test, $P < 10^{-4}$). Although the *mid-1* mutant maintained a lower turgor poise, it was capable of regulating turgor after a hyperosmotic treatment (Fig. 5). The growth rates of the wild type and the

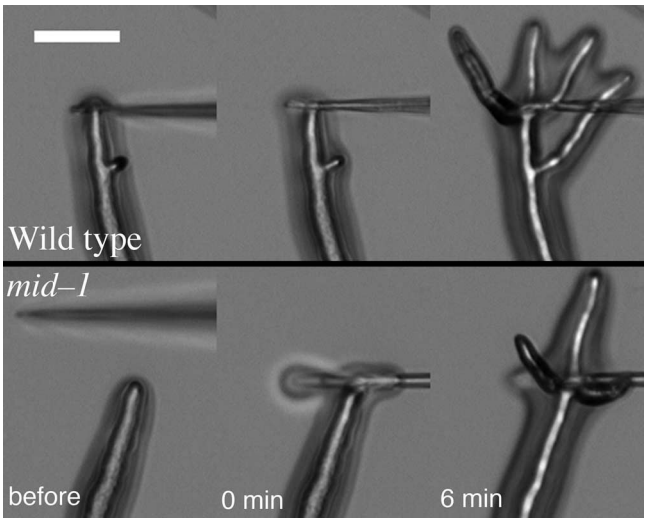

FIG. 4. Hyphal tip responses to a mechanical stimulus. A micropipette was appressed onto a growing hyphal tip, and responses were recorded every 90 s using time-lapse imaging. Typical examples of the response of wild type (upper panels) and *mid-1* mutant (lower panels) are shown before and immediately after the tip was appressed onto the hyphal tip, as well as 6 min later. Images were taken with a ×10 objective of hyphae growing on the surface of agar. Bar, 40 μm.

mid-1 mutant were compared at various concentrations of either sucrose or NaCl (Fig. 6). The *mid-1* mutant exhibited lower growth than the wild type at all osmoticum concentrations, and a growth decline at higher NaCl concentrations, but less sensitivity when sucrose was the osmoticum.

Hyperosmotically induced electrical responses of the *mid-1* mutant mirror wild-type responses. The electrical responses to hyperosmotic treatment were measured as described in previous work (20–22). Immediately after hyperosmotic treatment, there is a transient change in the potential, followed by a sustained hyperpolarization. The sustained hyperpolarization is caused by activation of the H^+-ATPase via the osmoresponsive mitogen-activated protein kinase cascade and occurs in concert with ion uptake to effect turgor recovery (21). The

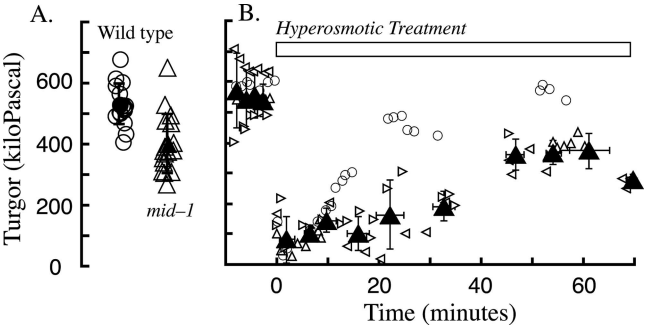

FIG. 5. Turgor and turgor recovery in the wild type and the *mid-1* mutant. (A) Turgor in the wild type (circles) was significantly higher than in the *mid-1* mutant (triangles). Data are jittered on the *x* axis for greater clarity. (B) Turgor recovery after addition of hyperosmotic solution at time 0. The wild type (circles) and the *mid-1* mutant (three separate experiments shown with open triangles of different orientations [means ± standard deviations are shown by filled triangles]) both exhibited turgor recovery after hyperosmotic treatment.

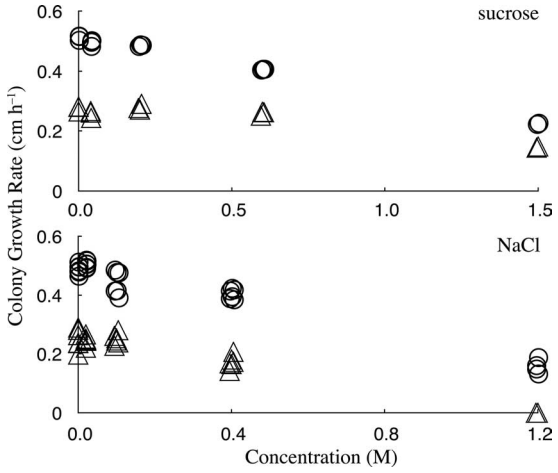

FIG. 6. Osmotic effects on growth of the wild type and the *mid-1* mutant. Shown are increases in colony diameters for the wild type (circles) and the *mid-1* mutant (triangles) at various concentrations of sucrose (upper panel) or NaCl (lower panel). Data are jittered on the *x* axis for clarity. Higher concentrations of sucrose were used to partially offset the difference in osmolarities of sucrose and NaCl. The osmolarities of the growth media at 0.6 M sucrose and 0.4 M NaCl were about 890 mmol kg^{-1} and 990 mmol kg^{-1}, respectively.

mid-1 mutant responds similarly (Fig. 7). It was notable that the transient change in potential immediately after hyperosmotic treatment, consistently a depolarization in the case of the wild type, was either a depolarization or hyperpolarization

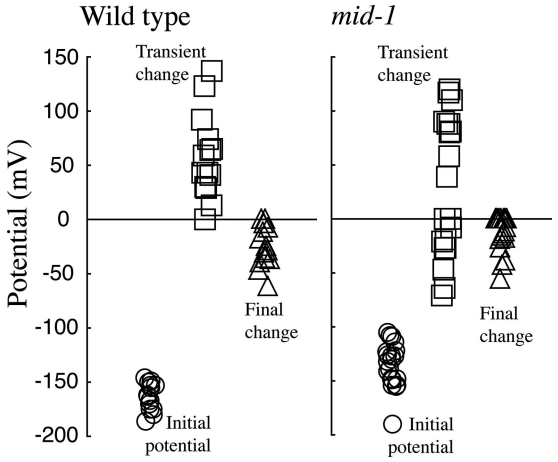

FIG. 7. Electrical responses of the wild type and the *mid-1* mutant to hyperosmotic treatment. The mycelial colony was flooded with 3 ml of BS; after about 15 min, when hyphal tips at the colony edge had resumed growth, hyphal trunk cells about 200 to 500 μm behind the colony edge were impaled with double-barrel microelectrodes. When the membrane potential had stabilized (circles) (initial potential), 0.5 ml of BS plus 1,000 mM sucrose was added in a circle around the microscope objective. Arrival of the hyperosmotic solution at the hypha being measured was confirmed by the observation of a refractive wave. A transient depolarization (transient change) (always observed in the wild type) or hyperpolarization (occasionally observed in the *mid-1* mutant [squares]) was observed within 2 min, followed by a long-term hyperpolarization (triangles) within 4 to 6 min. The transient and final changes respectively, are the transient potential or final potential minus the initial potential. Data are jittered on the *x* axis for clarity.

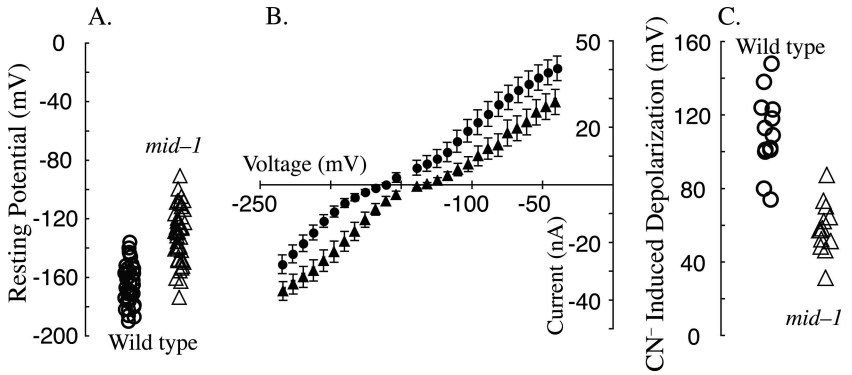

FIG. 8. Electrical properties of the wild type (circles) and the *mid-1* mutant (triangles). The resting potential (A) was significantly more negative in the wild type. Current-voltage relationships (B) exhibited similar conductances. Cyanide (CN^-)-induced depolarizations (C) were used to measure the activity of the ATP-dependent H^+-ATPase, which was significantly lower in the *mid-1* mutant than in the wild type. For panels A and C, data are jittered on the *x* axis for clarity.

in the *mid-1* mutant. The difference in the transient response was not statistically significant based on nonparametric tests (Kruskal-Wallis and Kolmogorov-Smirnof). In both the *mid-1* mutant and the wild type, the presence of a sustained hyperpolarization indicates that the regulation of ion fluxes underlying turgor recovery is unaffected in the *mid-1* mutant.

Since turgor is a driving force for cellular expansion, the lower turgor poise of the *mid-1* mutant may be the cause of its lower growth rate. The cause of lower turgor could be less ion accumulation during growth, which may be reflected by differences in electrical properties under normal conditions.

The *mid-1* mutant's potential is depolarized compared to the wild type due to lower H^+-ATPase activity. The wild-type potential was -164 ± 13 mV ($n = 39$), but the *mid-1* mutant was significantly more positive (-131 ± 18 mV; $n = 47$) (two-tailed *t* test, $P < 10^{-14}$) (Fig. 8A). The chord conductances near the resting potential (-200 to -50 mV) were very similar for both the wild type (323 nS, $n = 15$) and the *mid-1* mutant (304 nS, $n = 17$) (Fig. 8B). The similar chord conductances suggest that the cause of the depolarized potential in the *mid-1* mutant may be due to lower H^+-ATPase activity. This was tested by examining the effect of ATP depletion using 5 mM NaCN treatment. In the wild type, cyanide (CN^-) depolarized the potential from -160 ± 14 to -47 ± 20 mV, a change of 113 ± 19 mV ($n = 13$). In the *mid-1* mutant, CN^- depolarized the potential from -130 ± 21 to -72 ± 20 mV, a change of 58 ± 14 mV ($n = 13$). The CN^--induced depolarization, an indirect measure of the activity of the H^+-ATPase, was significantly less in the *mid-1* mutant (two-tailed *t* test, $P < 10^{-7}$). Thus, the lower potential of the *mid-1* mutant appears to be due to lower H^+-ATPase activity; this may be the cause of lower turgor in the *mid-1* mutant and thus its poor growth vigor.

DISCUSSION

In *Saccharomyces cerevisiae*, the *mid-1* mutant was initially identified on the basis of cell death when shmoos were formed during mating (10). Ca^{2+} influx was impaired in the mutant, and the mating-induced death phenotype was rescued by supplementing calcium in the growth medium. We did not observe this phenotype in the filamentous fungus *Neurospora crassa*. Mating, measured as viable ascospore production after crossing *mid-1* mating type *A* and *mid-1* mating type *a*, was very similar to control crosses of wild-type mating types *A* and *a*.

The yeast Mid1p product was identified as a stretch-activated channel based on patch clamp measurements after heterologous expression in mammalian CHO cells (11). Stretch-activated channels in hyphal organisms are inhibited by gadolinium (8, 36, 37). In both the rust fungus *Uromyces appendiculatus* (37) and the yeast *Candida albicans* (36), gadolinium also inhibits growth responses to mechanical barriers. So, an alternative role of Mid1p may be thigmotropism. This has been documented in *C. albicans* by Brand et al. (3), who found that the response of the hyphal form of the yeast *mid1* mutant to mechanical barriers was less than the wild-type response. Thigmotropic responses in *Aspergillus niger* are only observed after the fungi are subjected to nutrient stress (2), so thigmotropism is not a consistent growth response in fungi. It is possible that changes in hyphal growth direction when encountering a mechanical barrier could arise from differences in localized expansion as membrane fuses at the expanding tip without mediation by a mechanosensitive channel. In *N. crassa*, the hyperbranching responses of the wild type and the *mid-1* mutant to mechanical barriers, created by growing the fungus between two layers of scratched cellophane, were similar. Direct mechanical stimulation, appressing a micropipette at the tip of the growing hypha, caused the same hyperbranching response in the wild type and the *mid-1* mutant. Mechanical impedance, created by growing the fungi in VM with various concentrations of agar, slowed the growth rates of the wild type and the *mid-1* mutant similarly. The immediate electrical responses to hyperosmotic treatment, a treatment that would affect hyphal volume and area (the measured decline in surface area was about 7 to 15%, which may affect the activity of stretch-activated channels), were similar as well. Thus, based on a variety of different experimental approaches, the *mid-1* mutant of *N. crassa* does not exhibit phenotypes (mating or thigmotropism) similar to that of either *S. cerevisiae* or *C. albicans*. Instead, in *N. crassa*, the most notable attributes of the *mid-1* mutant are its slower growth and lower vigor under all conditions examined.

A broad comparison of growth rates on a variety of substrates revealed that nutrient utilization is unlikely to be the

cause of slower growth. The poor vigor does not affect the timing of the developmental patterns (conidiation) implicit in the circadian rhythm. Furthermore, hyphal cytology and mycelial processes such as hyphal flow and anastomoses are very similar in the wild type and the *mid-1* mutant. There was no indication of lesions in response to hyperosmotic treatment—turgor regulation, growth responses, and electrical responses—suggesting that signal transduction, at least of the osmotic mitogen-activated protein kinase cascade (21), is unaffected. Nevertheless, normal turgor was lower than in the wild type. This could cause lower growth since internal hydrostatic pressure is an important component of the forces contributing to cellular expansion (20). Ion uptake plays a role in maintenance of turgor (21). The two attributes of the *mid-1* mutant which exhibit "poor vigor" are electrical properties and turgor; both were lower than in the wild type. The depolarized potential of the *mid-1* mutant appears to be caused by lower H^+-ATPase activity in the mutant, based upon cyanide inhibition of respiration to dissect out the component of the membrane potential generated by the H^+-ATPase. This is the likely cause of the lower growth vigor of the mutant.

In the yeast *C. albicans*, the *mid1* mutant exhibits aberrant colony morphology, partially rescued by replete exogenous calcium (3), but elevated exogenous calcium did not rescue the slower growth of the *mid-1* mutant in *N. crassa*. Under normal growing conditions, the *mid-1* mutant's hyphal tip cytology was the same as that of the wild type, suggesting that the tip-high Ca^{2+} gradient required for growth (33) was operating normally. However, the mutant was unable to grow at either lower extracellular Ca^{2+} or elevated intracellular Ca^{2+}. Sensitivity to low Ca^{2+} has also been observed for the *S. cerevisiae mid1* mutant (23). Elevation of intracellular Ca^{2+} with the ionophore A23187 inhibited growth completely in the *N. crassa* mutant, resulting in a zone of exclusion where A23187 had been applied. The response in the wild type was more complex. Although it grew through the A23187 zone, hyperbranching, the elevated intracellular Ca^{2+} appeared to cause retrograde signaling, such that conidiation was inhibited in a sector extending back to the site of inoculation. In the *mid-1* mutant, the hypersensitivity to either low exogenous or elevated intracellular Ca^{2+} is consistent with an inability to regulate Ca^{2+} to maintain a homeostatic level in support of cellular processes regulated through Ca^{2+} signaling systems.

We propose that in *N. crassa*, MID-1 plays a role in Ca^{2+} homeostasis. In its absence, the filamentous fungus is unable to response normally to either lower or higher Ca^{2+} levels. The Ca^{2+} in turn may regulate ion transport activity, possibly modulating H^+-ATPase activity (16). In the absence of normal ion transport activity, turgor is lower, causing the slower growth and poor vigor of the *mid-1* mutant.

ACKNOWLEDGMENTS

Very special thanks goes to Patricia Lakin-Thomas and Sanshu Li (York University, Department of Biology) for guidance and assistance with circadian rhythm determinations and to Shanar Nasserifar and Karen Rethoret for contributions to fluorescence imaging.

The research was funded in part by a Discovery grant from the Natural Sciences and Engineering Research Council of Canada (to R.R.L.).

REFERENCES

1. **Bistis, G. N., D. D. Perkins, and N. D. Read.** 2003. Different cell types in *Neurospora crassa*. Fungal Genet. Newsl. **50:**17–19.
2. **Bowen, A. D., F. A. Davidson, R. Keatch, and G. M. Gadd.** 2007. Induction of contour sensing in *Aspergillus niger* by stress and its relevance to fungal growth mechanics and hyphal tip structure. Fungal Genet. Biol. **44:**484–491.
3. **Brand, A., S. Shanks, V. M. S. Duncan, M. Yang, K. Mackenzie, and N. A. R. Gow.** 2007. Hyphal orientation of *Candida albicans* is regulated by a calcium-dependent mechanism. Curr. Biol. **17:**347–352.
4. **Colot, H. V., G. Park, G. E. Turner, C. Ringelberg, C. M. Crew, L. Litvinkova, R. L. Weiss, K. A. Borkovich, and J. C. Dunlap.** 2006. A high through-put gene knockout procedure for *Neurospora* reveals functions for multiple transcription factors. Proc. Natl. Acad. Sci. USA **103:**10352–10357.
5. **Dutta, R., and K. R. Robinson.** 2004. Identification and characterization of stretch-activated ion channels in pollen protoplasts. Plant Physiol. **135:**1398–1406.
6. **Fischer-Parton, S., R. M. Parton, P. C. Hickey, J. Dijksterhuis, H. A. Atkinson, and N. D. Read.** 2000. Confocal microscopy of FM4-64 as a tool for analysing endocytosis and vesicle trafficking in living fungal hyphae. J. Microsc. **198:**246–259.
7. **Garrill, A., R. R. Lew, and I. B. Heath.** 1992. Stretch-activated Ca^{2+} and Ca^{2+}-activated K^+ channels in the hyphal tip plasma membrane of the oomycete *Saprolegnia ferax*. J. Cell Sci. **101:**721–730.
8. **Garrill, A., S. L. Jackson, R. R. Lew, and I. B. Heath.** 1993. Ion channel activity and tip growth: tip-localized, stretch-activated channels generate a Ca^{2+} gradient that is required for tip growth in the oomycete *Saprolegnia ferax*. J. Eur. Cell Biol. **60:**358–365.
9. **Hickey, P. C., D. J. Jacobson, N. D. Read, and N. L. Glass.** 2002. Live-cell imaging of vegetative hyphal fusion in *Neurospora crassa*. Fungal Genet. Biol. **37:**109–119.
10. **Iida, H., H. Nakamura, T. Ono, M. S. Okumura, and Y. Anraku.** 1994. *MID1*, a novel *Saccharomyces cerevisiae* gene encoding a plasma membrane protein, is required for Ca^{2+} influx and mating. Mol. Cell. Biol. **14:**8259–8271.
11. **Kanizaki, M., M. Nagasawa, I. Kojima, C. Sato, K. Naruse, M. Sokabe, and H. Iida.** 1999. Molecular identification of a eukaryotic, stretch-activated nonselective cation channel. Science **285:**882–886.
12. **Lakin-Thomas, P. L.** 1992. Phase resetting on the *Neurospora crassa* circadian oscillator: effects of inositol depletion on sensitivity to light. J. Biol. Rhythms **7:**227–239.
13. **Lakin-Thomas, P. L.** 1996. Effects of choline depletion on the circadian rhythm in *Neurospora crassa*. Biol. Rhythms Res. **27:**12–30.
14. **Levina, N. N., R. R. Lew, G. J. Hyde, and I. B. Heath.** 1995. The roles of calcium ions and plasma membrane ion channels in hyphal tip growth of *Neurospora crassa*. J. Cell Sci. **108:**3405–3417.
15. **Levina, N. N., and R. R. Lew.** 2006. The role of tip-localized mitochondria in hyphal growth. Fungal Genet. Biol. **43:**65–74.
16. **Lew, R. R.** 1989. Calcium activates an electrogenic proton pump in *Neurospora* plasma membrane. Plant Physiol. **91:**213–216.
17. **Lew, R. R.** 1996. Pressure regulation of the electrical properties of growing *Arabidopsis thaliana* L. roothairs. Plant Physiol. **112:**1089–1100.
18. **Lew, R. R.** 2006. Use of double barrel micropipettes to voltage-clamp plant and fungal cells, p. 139–154. *In* A. G. Volkov (ed.), Plant electrophysiology—theory and methods. Springer, Berlin, Germany.
19. **Lew, R. R.** 2007. Ionic currents and ion fluxes in *Neurospora crassa*. J. Exp. Bot. **58:**3475–3481. doi:10.1093/jxb/erm204.
20. **Lew, R. R., N. N. Levina, S. K. Walker, and A. Garrill.** 2004. Turgor regulation of hyphal organisms. Fungal Genet. Biol. **41:**1007–1015.
21. **Lew, R. R., N. N. Levina, L. Shabala, M. I. Anderca, and S. N. Shabala.** 2006. Role of a mitogen-activated protein kinase cascade in ion flux-mediated turgor regulation in fungi. Eukaryot. Cell **5:**480–487.
22. **Lew, R. R., and N. N. Levina.** 2007. Turgor regulation in the osmosensitive *cut* mutant of *Neurospora crassa*. Microbiology **153:**1530–1537.
23. **Liu, M., P. Du, G. Heinrich, G. M. Cox, and A. Gelli.** 2006. Cch1 mediates calcium entry in *Cryptococcus neoformans* and is essential in low-calcium environments. Eukaryot. Cell **5:**1788–1796.
24. **Maruoka, T., Y. Nagasoe, S. Inoue, Y. Mori, J. Goto, M. Ikeda, and H. Iida.** 2002. Essential hydrophilic carboxyl-terminal regions including cysteine residues of the yeast stretch-activated calcium-permeable channel mid1. J. Biol. Chem. **277:**11645–11652.
25. **McCluskey, K.** 2003. The Fungal Genetics Stock Center: from molds to molecules. Adv. Appl. Microbiol. **52:**245–262.
26. **Nakagawa, Y., T. Katagiri, K. Shinozaki, Z. Qi, H. Tatsumi, T. Furuichi, A. Kishigami, M. Sokabe, I. Kojima, S. Sato, T. Kato, S. Tabata, K. Iida, A. Terashima, M. Nakano, M. Ikeda, T. Yamanaka, and H. Iida.** 2007. *Arabidopsis* plasma membrane protein crucial for Ca^{2+} influx and touch-sensing in roots. Proc. Natl. Acad. Sci. USA **104:**3639–3644.
27. **Nelson, G., O. Kozlova-Zwinderman, A. J. Collis, M. R. Knight, J. R. S. Fincham, C. P. Stanger, A. Renwick, J. G. M. Hessing, P. J. Punt, C. A. M. J. J. van den Hondel, and N. D. Read.** 2004. Calcium measurement in living filamentous fungi expressing codon-optimized aequorin. Mol. Microbiol. **52:**1437–1450.

28. **Ozeki-Miyawaki, C., Y. Moriya, H. Tatsumi, H. Iida, and M. Sokabe.** 2005. Identification of functional domains of Mid1, a stretch-activated channel component, necessary for localization to the plasma membrane and Ca^{2+} permeation. Exp. Cell Res. **311:**84–95.
29. **Paidhungat, M., and S. Garrett.** 1997. A homolog of mammalian, voltage-gated calcium channels mediates yeast pheromone-stimulated Ca^{2+} uptake and exacerbates the *cdc1*(Ts) growth defect. Mol. Cell. Biol. **17:**6339–6347.
30. **Reissig, J. L., and S. G. Kinney.** 1983. Calcium as a branching signal in *Neurospora crassa*. J. Bacteriol. **154:**1397–1402.
31. **Riquelme, M., R. W. Roberson, D. P. McDaniel, and S. Bartnicki-Garcia.** 2002. The effects of ropy-1 mutation on cytoplasmic organization and intracellular motility in mature hyphae of *Neurospora crassa*. Fungal Genet. Biol. **37:**171–179.
32. **Robinson, W. B., A. E. Mealor, S. E. Stevens, Jr., and M. Ospeck.** 2007. Measuring the force production of the homogonia of *Mastigocladus laminosus*. Biophys. J. **93:**699–703.
33. **Silverman-Gavrila, L. B., and R. R. Lew.** 2002. An IP_3-activated Ca^{2+} channel regulates fungal tip growth. J. Cell Sci. **115:**5013–5025.
34. **Trinci, A. P. J.** 1973. The hyphal growth unit wild type and spreading colonial mutants of *Neurospora crassa*. Arch. Mikrobiol. **91:**127–136.
35. **Vogel, H. J.** 1956. A convenient growth medium for *Neurospora*. Microb. Genet. Bull. **13:**42–46.
36. **Watts, H. J., A. A. Very, T. H. Perera, J. M. Davies, and N. A. Gow.** 1998. Thigmotropism and stretch-activated channels in the pathogenic fungus *Candida albicans*. Microbiology **144:**689–695.
37. **Zhou, X. L., M. A. Stumpf, H. C. Hoch, and C. Kung.** 1991. A mechanosensitive channel in whole cells and in membrane patches of the fungus *Uromyces*. Science **253:**1415–1417.